NUMERICAL SIMULATION OF TRANSITIONAL FLOWS WITH LAMINAR KINETIC ENERGY

Jiří Fürst*

The article deals with the numerical solution of transitional flows. The single-point k-k_L-ω model of [7] based on the use of a laminar kinetic energy transport equation is considered. The model doesn't require to evaluate integral boundary layer parameters (e.g. boundary layer thickness) and is therefore suitable for implementation into codes working with general unstructured meshes. The performance of the model has been tested for the case of flows over a flat plate with zero and non-zero pressure gradients. The results obtained with our implementation of the model are compared to the experimental data of ERCOFTAC.

Keywords: *turbulence, transition, Navier-Stokes equations*

1. Introduction

The laminar-turbulent transition plays very important role in many flows of engineering interest. It has big impact on the heat transfer and losses. Unfortunately most of the state of the art turbulence models (e.g. Menters SST k-ω model, EARSM model of Hellsten) completely fail with the prediction of transition. However there are some attempts to modify basic models (e.g. low-Reynolds model of [12], the k-ω model with total stress limiter proposed by [13]) with promising results, the experience shows that this approach is not capable of reliably capturing all factors that affect transition, see [6].

The algebraic models based on empirical correlations (see e.g. [8]) offers simple approach with sufficient accuracy. On the other hand their implementation into a general unstructured code is quite difficult due to necessity of some non-local information (momentum boundary layer thickness, etc.). Therefore the applicability of these models is more-less limited to research or academic codes using structured meshes.

This article deals with the RANS-based transitional model developed by [9]. The three-equation model is based on the low-Reynolds k-ω model with an equation for the so called laminar kinetic energy k_L expressing the energy of stream-wise fluctuations in pre-transitional region.

The concept of laminar kinetic energy proposed by Mayle and Schulz [5] follows from the physical description of the transition process, see e.g. [7]. During the transition the laminar boundary layer becomes unstable at certain Ryenolds number and the primary instabilities (the Tollmien-Schlichting waves) occur. Due to secondary instabilities the three-dimensional disturbances are superimposed further downstream. These lead to the so called Λ-vortices which are later replaced by the turbulent spots, which initiate the transition. Turbulent

* doc. Ing. J. Fürst, PhD.: Fac. of Mech. Eng., Czech Technical University in Prague, Karlovo nám. 13; 121 35, Prague; CZ

spots grow until the the flow is fully turbulent. It is important to note that the fluctuations in the pre-transitional part of the boundary layer (i.e. the part starting with the primary instabilities and ending with to the formation of turbulent spots) are not turbulence in the usual sense of that word. Therefore Mayle and Schulz [5] proposed the adoption of the laminar kinetic energy equation to describe the evolution of these fluctuations. For more detailed description of the model including other modes of transition please see [10] or [9].

The main advantage of the model is its local formulation, it means that it can be easily implemented into unstructured solvers. Moreover it can (at least in principle) handle flows in complex geometry. Unfortunately the description of the model in [9] contains some errors (probably typos) which lead to strong underestimation of the friction in turbulent region. The aim of the article is to describe the correct version of the model and to test the performance of the model for simple flows over flat plate.

2. Mathematical model

2.1. Navier-Stokes equations

The viscous compressible flows are described by the set of Favre-averaged Navier-Stokes equations:

$$\frac{\partial \rho}{\partial t} + \frac{\partial (\rho\, u_j)}{\partial x_j} = 0 \ , \tag{1}$$

$$\frac{\partial (\rho u_i)}{\partial t} + \frac{\partial (\rho\, u_i\, u_j)}{\partial x_j} + \frac{\partial p}{\partial x_i} = \frac{\partial (t_{ij} + \tau_{ij})}{\partial x_j} \ , \tag{2}$$

$$\frac{\partial (\rho E)}{\partial t} + \frac{\partial [(\rho\, E + p)\, u_j]}{\partial x_j} = \frac{\partial}{\partial x_j} \left[u_i\, (t_{ij} + \tau_{ij}) + \left(\frac{\mu}{Pr} + \rho\, \alpha_\theta \right) \frac{\partial h}{\partial x_j} \right] \ , \tag{3}$$

where ρ is the density, u_i are the components of the velocity vector, p is the static pressure, E is the specific total energy, $h = E + p - u_i\, u_i/2$ is the specific enthalpy, t_{ij} is the mean viscous stress tensor, $\tau_{ij} = -\overline{\rho\, u_i'\, u_j'}$ is the Reynolds stress tensor, μ is the viscosity, Pr is the Prandtl number, and α_θ is the turbulent thermal diffusivity.

We assume perfect gas (the air) with $p = (\kappa - 1)(\rho\, E - \rho\, u_i\, u_i/2)$ where $\kappa = 1.4$ is the constant specific heat ratio. The flow is Newtonian with constant viscosity μ, hence $t_{ij} = 2\, \mu\, (S_{ij} - S_{ll}\, \delta_{ij}/3)$ where $S_{ij} = (\partial u_i/\partial x_j + \partial u_j/\partial x_i)/2$.

2.2. Turbulence model

The turbulence model is based on the Boussinesq hypothesis

$$\tau_{ij} = 2\, \rho\, \nu_{\mathrm{T}} \left(S_{ij} - \frac{1}{3}\, S_{ll}\, \delta_{ij} \right) - \frac{1}{3}\, \rho\, k\, \delta_{ij} \ , \tag{4}$$

where ν_{T} is the turbulent kinematic viscosity and k is the turbulent kinetic energy.

We assume a three equation model of [9] with the transport equations for the turbulent kinetic energy k_{T}, the laminar kinetic energy k_{L}, and the specific dissipation rate ω. The equations are

$$\frac{D(\rho\, k_{\mathrm{T}})}{Dt} = \rho\, (P_{k_{\mathrm{T}}} + R_{\mathrm{BP}} + R_{\mathrm{NAT}} - \omega\, k_{\mathrm{T}} - D_{\mathrm{T}}) + \frac{\partial}{\partial x_j} \left[\left(\mu + \frac{\rho\, \alpha_{\mathrm{T}}}{\sigma_k} \right) \frac{\partial k_{\mathrm{T}}}{\partial x_j} \right] \ , \tag{5}$$

$$\frac{D(\rho\, k_{\mathrm{L}})}{Dt} = \rho\,(P_{k_{\mathrm{L}}} - R_{\mathrm{BP}} - R_{\mathrm{NAT}} - D_{\mathrm{L}}) + \frac{\partial}{\partial x_j}\left[\mu\,\frac{\partial k_{\mathrm{L}}}{\partial x_j}\right]\,, \tag{6}$$

$$\begin{aligned}\frac{D(\rho\,\omega)}{Dt} = \rho\Bigg[C_{\omega 1}\,\frac{\omega}{k_{\mathrm{T}}}\,P_{k_{\mathrm{T}}} + \left(\frac{C_{\omega \mathrm{R}}}{f_{\mathrm{W}}} - 1\right)\frac{\omega}{k_{\mathrm{T}}}\,(R_{\mathrm{BP}} + R_{\mathrm{NAT}}) - C_{\omega 2}\,\omega^2 + \\ + C_{\omega 3}\,f_\omega\,\alpha_{\mathrm{T}}\,f_{\mathrm{W}}^2\,\frac{\sqrt{k_{\mathrm{T}}}}{d^3}\Bigg] + \frac{\partial}{\partial x_j}\left[\left(\mu + \frac{\rho\,\alpha_{\mathrm{T}}}{\sigma_\omega}\right)\frac{\partial \omega}{\partial x_j}\right]\,.\end{aligned} \tag{7}$$

The various terms in the equations represents production, destruction, transport, and diffusion. However the structure of the model is more-less clear, there is a confusion in the definition of individual terms in the literature. The original Walters and Leylek's model (see [10]) uses k_{T}-k_{L}-ϵ formulation. The model was later re-formulated using k_{T}-k_{L}-ω (see [11] or [4]) and the current version was published in [9]. Unfortunately it seems that the last article contains some errors. Therefore we will write here all individual terms and we will comment the differences of our version with respect to the original article.

The production of turbulent and laminar kinetic energy is

$$P_{k_{\mathrm{T}}} = \nu_{\mathrm{T,s}}\,S^2\,, \tag{8}$$

$$P_{k_{\mathrm{L}}} = \nu_{\mathrm{T,l}}\,S^2\,, \tag{9}$$

where $S = \sqrt{2\,S_{ij}\,S_{ij}}$. The 'small-scale' eddy viscosity is defined as

$$\nu_{\mathrm{T,s}} = f_\nu\,f_{\mathrm{INT}}\,C_\mu\,\sqrt{k_{\mathrm{T,s}}}\,\lambda_{\mathrm{eff}}\,, \tag{10}$$

where $k_{\mathrm{T,s}}$ is the effective small-scale turbulence

$$k_{\mathrm{T,s}} = f_{\mathrm{SS}}\,f_{\mathrm{W}}\,k_{\mathrm{T}}\,. \tag{11}$$

The wall-limited turbulence length scale λ_{eff} and damping function f_{W} is

$$\lambda_{\mathrm{eff}} = \min(C_\lambda\,d, \lambda_{\mathrm{T}})\,, \tag{12}$$

$$\lambda_{\mathrm{T}} = \frac{\sqrt{k_{\mathrm{T}}}}{\omega}\,, \tag{13}$$

$$f_{\mathrm{W}} = \left(\frac{\lambda_{\mathrm{eff}}}{\lambda_{\mathrm{T}}}\right)^{\frac{2}{3}}\,, \tag{14}$$

here d is the wall distance. Note that the article [9] does not include the exponent 2/3 in the definition of f_{W}. The original model [10] as well as the [11] do include the exponent. The origins of the 2/3 exponent come from the k-ϵ formulation where the turbulent length scale is

$$\lambda_{\mathrm{T}} = \frac{k_{\mathrm{T}}^{\frac{3}{2}}}{\epsilon}\,, \tag{15}$$

therefore f_{W} actually limits the length scale to λ_{eff}.

The following terms are according to [9]

$$f_\nu = 1 - \exp\left(-\frac{\sqrt{Re_{\mathrm{T}}}}{A_\nu}\right)\,, \tag{16}$$

$$Re_{\mathrm{T}} = \frac{f_{\mathrm{W}}^2\, k_{\mathrm{T}}}{\nu\, \omega} \ , \tag{17}$$

$$f_{\mathrm{SS}} = \exp\left[- \left(\frac{C_{\mathrm{ss}}\, \nu\, \Omega}{k_{\mathrm{T}}} \right)^2 \right] \ , \tag{18}$$

$$C_{\mu} = \frac{1}{A_0 + A_{\mathrm{S}} \left(\dfrac{S}{\omega} \right)} \ . \tag{19}$$

The intermittency factor f_{INT} is

$$f_{\mathrm{INT}} = \min \left(\frac{k_{\mathrm{T}}}{C_{\mathrm{INT}}\, (k_{\mathrm{T}} + k_{\mathrm{L}})} \ , 1 \right) \ . \tag{20}$$

Note that the factor f_{INT} is defined with k_{L} in nominator in [9], but the article [11] gives correct form with k_{T}.

The production of laminar kinetic energy k_{L} is assumed to be given by large-scale near wall turbulence

$$k_{\mathrm{T,l}} = k_{\mathrm{T}} - k_{\mathrm{T,s}} \ . \tag{21}$$

The production term is then given by the equation (9) where

$$\nu_{\mathrm{T,l}} = \min \left\{ f_{\tau,\mathrm{l}}\, C_{\mathrm{l}1}\, \frac{\Omega\, \lambda_{\mathrm{eff}}^2}{\nu}\, \sqrt{k_{\mathrm{T,l}}}\, \lambda_{\mathrm{eff}} + \beta_{\mathrm{TS}}\, C_{\mathrm{l}2}\, Re_{\Omega}\, d^2\, \Omega, \frac{k_{\mathrm{L}} + k_{\mathrm{T,l}}}{2\, S} \right\} \ . \tag{22}$$

Here

$$Re_{\Omega} = \frac{d^2\, \Omega}{\nu} \ , \tag{23}$$

$$\beta_{\mathrm{TS}} = 1 - \exp \left(- \frac{\max(Re_{\Omega} - C_{\mathrm{TS,crit}}, 0)^2}{A_{\mathrm{TS}}} \right) \ , \tag{24}$$

$$f_{\tau,\mathrm{l}} = 1 - \exp \left(- C_{\tau,\mathrm{l}} \frac{k_{\tau_{\mathrm{l}}}}{\lambda_{\mathrm{eff}}^2\, \Omega^2} \right) \ . \tag{25}$$

The dissipation rate ϵ_{Tot} is divided to an isotropic ($k_{\mathrm{T}}\, \omega$) and anisotropic ($D_{\mathrm{T/L}}$) part (similarly as in the low-Reynolds Launder and Sharma k-ϵ model) with

$$D_{\mathrm{T}} = \nu\, \frac{\partial \sqrt{k_{\mathrm{T}}}}{\partial x_i}\, \frac{\partial \sqrt{k_{\mathrm{T}}}}{\partial x_i} \ , \tag{26}$$

$$D_{\mathrm{L}} = \nu\, \frac{\partial \sqrt{k_{\mathrm{L}}}}{\partial x_i}\, \frac{\partial \sqrt{k_{\mathrm{L}}}}{\partial x_i} \ . \tag{27}$$

However the the balance between the dissipation rate ϵ_{Tot} and diffusion $\partial(\nu\, \partial k_{\mathrm{T/L}}/\partial y)/\partial y$ in the laminar sublayer suggests the same formula multiplied by 2 (see e.g. Launder-Sharma k-ϵ model or the older versions of k-k_{L}-ϵ and k-k_{l}-ω) model, the above mentioned form was proposed in the new model and used in our calculations.

The turbulent diffusivity α_{T} is

$$\alpha_{\mathrm{T}} = f_{\nu}\, C_{\mu,\mathrm{std}}\, \sqrt{k_{\mathrm{T,s}}}\, \lambda_{\mathrm{eff}} \ , \tag{28}$$

and the damping function f_ω is

$$f_\omega = 1 - \exp\left[-0.41\left(\frac{\lambda_{\text{eff}}}{\lambda_{\text{T}}}\right)^4\right] \ . \tag{29}$$

The remaining terms R_{BP} and R_{NAT} express the laminar-turbulent transition in terms of the energy transfer from k_{L} to k_{T}. They are of the form

$$R_{\text{BP}} = \frac{C_{\text{R}}\,\beta_{\text{BP}}\,k_{\text{L}}\,\omega}{f_{\text{W}}} \ , \tag{30}$$

$$R_{\text{NAT}} = C_{\text{R,NAT}}\,\beta_{\text{NAT}}\,k_{\text{L}}\,\Omega \ . \tag{31}$$

The bypass transition is driven by the β_{BP} function

$$\beta_{\text{BP}} = 1 - \exp\left(-\frac{\phi_{\text{BP}}}{A_{\text{BP}}}\right) \ , \tag{32}$$

$$\phi_{\text{BP}} = \max\left(\frac{k_{\text{T}}}{\nu\,\Omega} - C_{\text{BP,crit}}, 0\right) \ , \tag{33}$$

and the natural transition by the β_{NAT} function

$$\beta_{\text{NAT}} = 1 - \exp\left(-\frac{\phi_{\text{NAT}}}{A_{\text{NAT}}}\right) \ , \tag{34}$$

$$\phi_{NAT} = \max\left(Re_\Omega - \frac{C_{\text{NAT,crit}}}{f_{\text{NAT,crit}}}, 0\right), \tag{35}$$

$$f_{\text{NAT,crit}} = 1 - \exp\left(-C_{\text{NC}}\,\frac{\sqrt{k_{\text{L}}}\,d}{\nu}\right) \ . \tag{36}$$

The turbulent kinematic viscosity used in the momentum equations is then

$$\nu_{\text{T}} = \nu_{\text{T,s}} + \nu_{\text{T,l}} \ . \tag{37}$$

The turbulent thermal diffusivity α_θ is then

$$\alpha_\theta = f_{\text{W}}\,\frac{k_{\text{T}}}{k_{\text{T}} + k_{\text{L}}}\,\frac{\nu_{\text{T,s}}}{Pr} + (1 - f_{\text{W}})\,C_{\alpha,\theta}\,\sqrt{k_{\text{T}}}\,\lambda_{\text{eff}} \ . \tag{38}$$

The coefficient $C_{\omega 2} = 0.92$ is constant in the original article. Nevertheless the correct form is

$$C_{\omega 2} = 0.92\,f_{\text{W}}^2 \ . \tag{39}$$

The other constants are

$$\begin{aligned}
A_0 &= 4.04 \ , & C_{\text{INT}} &= 0.75 \ , & C_{\omega 1} &= 0.44 \ , \\
A_{\text{S}} &= 2.12 \ , & C_{\text{TS,crit}} &= 1000 \ , & C_{\omega 3} &= 0.3 \ , \\
A_\nu &= 6.75 \ , & C_{\text{R,NAT}} &= 0.02 \ , & C_{\omega\text{R}} &= 1.5 \ , \\
A_{\text{BP}} &= 0.6 \ , & C_{l1} &= 3.4{\times}10^{-6} \ , & C_\lambda &= 2.495 \ , \\
A_{\text{NAT}} &= 200 \ , & C_{l2} &= 10^{-10} \ , & C_{\mu,\text{std}} &= 0.09 \ , \\
A_{\text{TS}} &= 200 \ , & C_R &= 0.12 \ , & Pr &= 0.85 \ . \\
C_{\text{BP,crit}} &= 1.2 \ , & C_{\alpha,\theta} &= 0.035 \ , & \sigma_k &= 1 \ , \\
C_{\text{NC}} &= 0.1 \ , & C_{\text{SS}} &= 1.5 \ , & \sigma_\omega &= 1.17 \ , \\
C_{\text{NAT,crit}} &= 1250 \ , & C_{\tau,\text{l}} &= 4360 \ .
\end{aligned}$$

3. Simulation of flows over a flat plate

The model has been validated using T3 series of experimental flat-plate test cases of ERCOFTAC. The T3A, T3B, and T3A- test cases had zero stream-wise pressure gradients with free-stream turbulence of 3%, 6%, and 1% respectively, see [1]. The T3C2 has favourable pressure gradient in the first part of the plate followed by the adverse pressure gradient in the second part, see [2].

The calculation was carried out with OpenFOAM package with our implementation of the k-k_L-ω model. The numerical solution was obtained with finite volume method using SIMPLEC scheme for compressible flows (see eg. [3]).

The zero-pressure gradient cases (i.e. T3A, T3A-, and T3B) were calculated using a rectangular domain $\Omega = [-0.05, 2.9] \times [0, 0.175]\,\mathrm{m}$ where the flat plate starts at $x = 0\,\mathrm{m}$. The mesh consists of 635×105 cells where 600 cells were at the plate and 35 cells in the inlet region. The mesh was refined in the vicinity of the inlet edge (see fig. 1) and in the wall normal direction with $y_1 \approx 10^{-5}\,\mathrm{m}$ i.e. $y^+ \leq 1$.

The following boundary conditions were prescribed:

inlet: at the inlet plane ($x = -0.05\,\mathrm{m}$) we prescribe the velocity vector u_i, the temperature ($T = 293.15\,\mathrm{K}$), the turbulent kinetic energy k_T, the laminar kinetic energy $k_\mathrm{L} = 0\,\mathrm{m^2\,s^{-2}}$, and the specific dissipation rate ω. The pressure is calculated with the homogeneous Neumann condition $\partial p/\partial n = 0$.

wall: at the wall ($x = 0\,\mathrm{m}$ to $2.9\,\mathrm{m}$ and $y = 0\,\mathrm{m}$) we prescribe non-slip condition for velocity ($u_i = 0\,\mathrm{m/s}$), the homogeneous Neumann condition for pressure $\partial p/\partial n = 0$, zero turbulent and laminar kinetic energy $k_\mathrm{T} = k_\mathrm{L} = 0\,\mathrm{m^2\,s^{-2}}$, and the homogeneous Neumann condition for the specific dissipation rate $\partial\omega/\partial n = 0$.

outlet: at the outlet ($x = 2.9\,\mathrm{m}$) we prescribe the static pressure $p = 101\,\mathrm{kPa}$ and we use homogeneous Neumann conditions for all remaining quantities.

symmetry: at the rest of the boundary (the upper boundary at $y = 0.175\,\mathrm{m}$ and the lower boundary in front of the plate) we assume symmetry condition for all variables (i.e. the slip condition).

We use constant dynamic viscosity $\mu = 1.8{\times}10^{-5}\,\mathrm{Pa\,s}$ and the ideal gas constant $R = 287\,\mathrm{J\,kg^{-1}\,K^{-1}}$. The parameters of inlet flows are are given in the table 1.

case	U [$\mathrm{m\,s^{-1}}$]	k_T [$\mathrm{m^2\,s^{-2}}$]	ω [$\mathrm{s^{-1}}$]	Tu [%]	$\mu_{\mathrm{T,std}}/\mu$ [–]
T3A	5.4	0.04763	23.8	3.30	12
T3B	9.2	1.12827	56.8	9.43	120
T3A-	19.8	0.04857	23.8	0.91	12
T3C2	5.5	0.05558	35.0	3.50	10

Tab.1: Inlet conditions for flat plate calculations at $x = -0.05\,m$, here $\mu_{\mathrm{T,std}} = C_{\mu,\mathrm{std}}\,\rho\,k_\mathrm{T}/\omega$

The figure 1 shows comparison of computed skin friction for T3A, T3B and T3A- cases with the experimental data of ERCOFTAC. One can see that the ready-made implementation of the model (labeled by OF 2.1.0 at the figure) fails even with T3A case. On the other hand our implementation of corrected model gives quite good agreement with experimental data from ERCOFTAC database. The results show that the transition onset is very

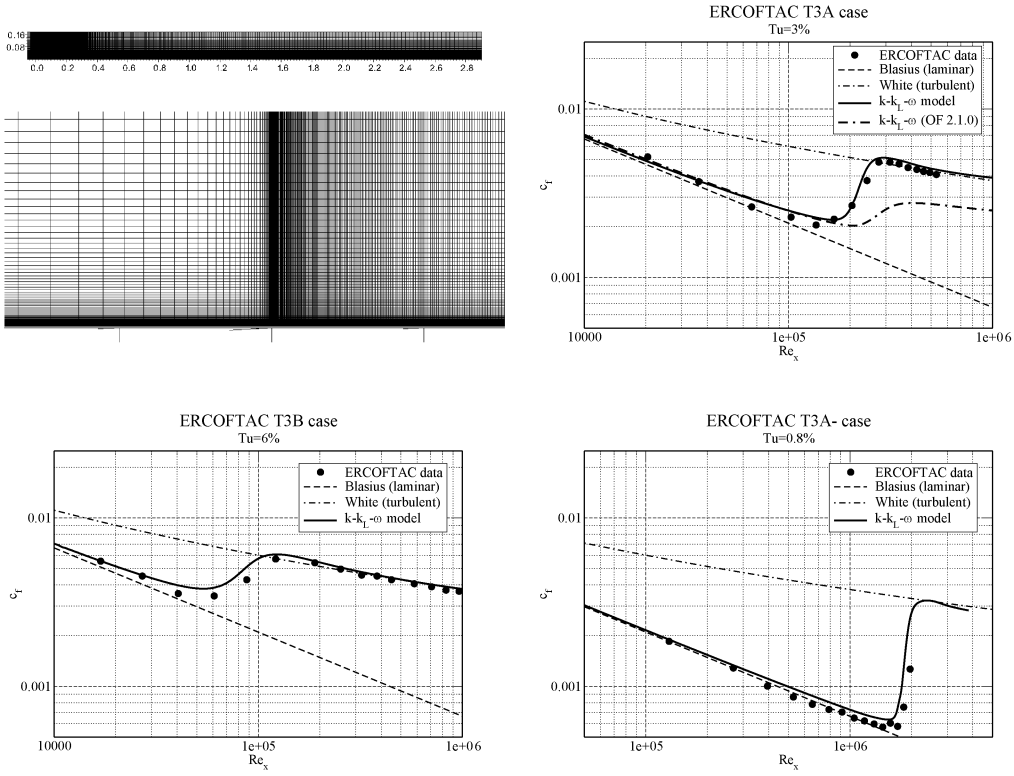

Fig.1: Friction coefficient for zero-pressure gradient flows over a flat plate (ERCOFTAC T3A, T3B, T3A- cases)

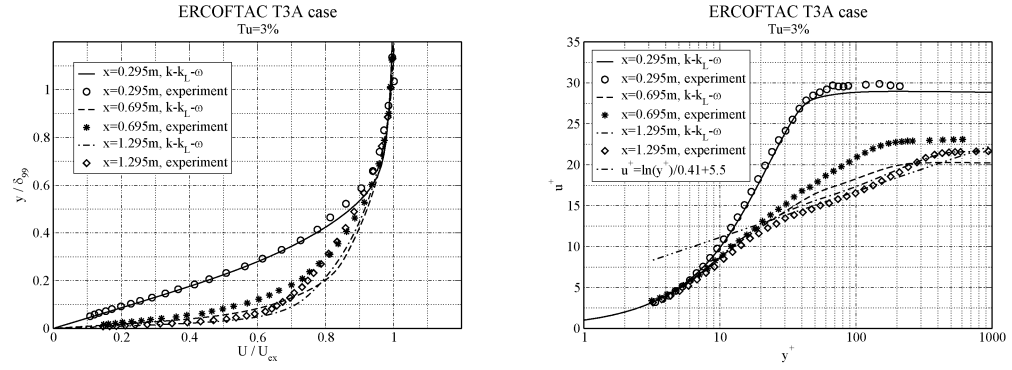

Fig.2: Velocity profiles at $x = 0.295$ m, 0.695 m, and 1.295 m for T3A case; comparison with ERCOFTAC data [1]

well captured in T3A and T3A- cases. In the T3B case with high turbulence intensity the transition seems to be shifted little bit upstream.

The figure 2 shows the comparison of velocity profiles at $x = 0.295\,\mathrm{m}$, $0.695\,\mathrm{m}$, and $1.295\,\mathrm{m}$ (i.e. $Re_\mathrm{x} \approx 100\,000$, $250\,000$ and $466\,000$). The comparison with experimental data [1] shows very good agreement of the computed velocity profile in laminar part of boundary layer ($x = 0.295\,\mathrm{m}$) and quite good agreement in turbulent part ($x = 0.295\,\mathrm{m}$).

The velocity profile is not very well captured in transitional part ($x = 0.695\,\mathrm{m}$). The figure 2 shows that the measured velocity at $x = 0.695\,\mathrm{m}$ obeys more-less standard logarithmic wall law for $40 < y^+ < 200$ whereas the calculated profile does not contain log-law profile at all. However we would like to note that it is very difficult to compare experimental data with numerical simulations in this case. The profiles in transitional part depend strongly on stream-wise position, free-stream turbulence intensity, and dissipation and therefore even relatively small error in each of these parameters can cause qualitative changes in velocity profiles.

The figure 3 (left) shows the profiles of kinetic energy $k_{\mathrm{Tot}} = k_{\mathrm{T}} + k_{\mathrm{L}}$ and the figure 3 (right) shows the evolution of maximum $k_{\mathrm{T,max}}(x) = \max_{\mathrm{y}} k(x, y)$ and $k_{\mathrm{L,max}}(x) = \max_{\mathrm{y}} k_{\mathrm{L}}(x, y)$ along the wall. The latest figure confirms the behaviour of the model:

- the laminar kinetic energy k_{L} grows almost linearly in the laminar part of the boundary layer,
- the laminar fluctuations change to turbulent one in the transitional part of the boundary layer (growth of k_{T} and diminution of k_{L}),
- the turbulent kinetic energy becomes dominant over k_{L} in turbulent part of the boundary layer ($k_{\max} \gg k_{\mathrm{L,max}}$).

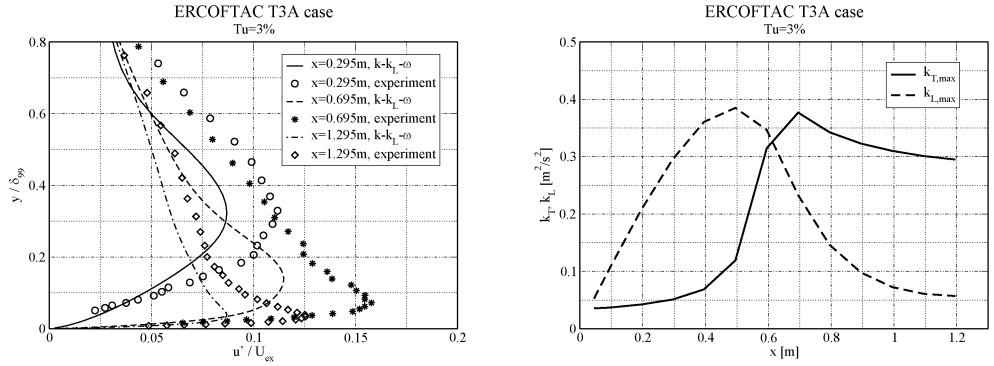

Fig.3: Profiles of turbulent kinetic energy at $x = 0.295\,\mathrm{m}$, 0.595 m, and 1.195 m (left) and the evolution of maximum of k_{T} and k_{L} along the wall (right) for T3A case

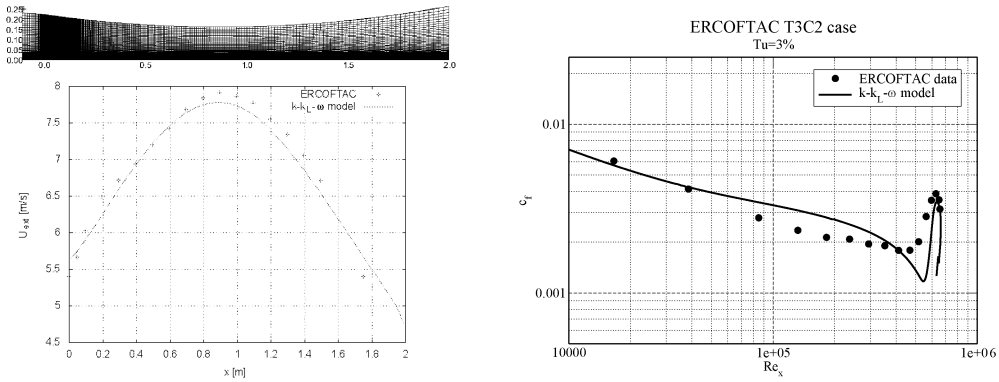

Fig.4: Domain, the velocity at $y = 0.05\,\mathrm{m}$ and the friction coefficient for T3C2 ERCOFTAC case

For the flow with pressure gradient (T3C2 case) we assume a domain with shaped upper boundary (see fig. 4). The shape was constructed in order to match the velocity distribution in the ERCOFTAC experiment. Fig. 4 shows the comparison of experimental data with the calculated velocity distribution at $y = 0.05\,\mathrm{m}$. The calculated skin friction coefficient* shows that the model predicts the transition onset to late. On the other hand the transition length is underpredicted, so the position of transition end is captured at right position.

4. Conclusion

Our results indicate that the model of [9] is able (after all necessary corrections with respect to the original article) to predict the laminar-turbulent transition for simple flows over flat plate. The model predicts very well the distribution of friction coefficient c_f as well as the velocity profiles in laminar and turbulent parts of the boundary layer (at least for the zero pressure gradient case). On the other hand it delays the transition onset for T3C2 case (flows with adverse pressure gradient).

Despite of the difficult correlations and many constants the model is compatible with modern unstructured CFD codes (e.g. with OpenFOAM) and it should be (at least in principle) able to calculate transitional flows in complex geometry.

Future work will be oriented to the implementation of the model to our in-house code and to its applications for flows in turbine cascades.

Acknowledgments

The work was supported by the Grant no. P101/10/1329 and P101/12/1271 of the Czech Science Foundation. The author would like to thank prof. K. Walters for the clarification of the model.

References

[1] Coupland J.: Ercoftac special interest group on laminar to turbulent transition and retransition: T3a and t3b test cases, Tech. rep., ERCOFTAC, 1990
[2] Coupland J.: Ercoftac special interest group on laminar to turbulent transition and retransition: T3c test cases, Tech. rep., ERCOFTAC, 1990
[3] Ferziger J.H., Peric M.: Computational Methods for Fluid Dynamics, Springer, 1999
[4] Holloway D.S., Walters D.K., Leylek J.D.: Prediction of unsteady, separated boundary layer over a blunt body for laminar, turbulent, and transitional flow, Int. Journal for Numerical Methods in Fluids 45 (2004), 1291–1315
[5] Mayle R.E., Schulz A.: The path to predicting bypass transition, ASME Journal of Turbomachinery, 119 (1997), 405–411
[6] Menter F.R., Langtry R.B., Likki S.R., Suzen Y.B., Huang P.G., Völker S.: A correlation-based transition model using local variables – Part I: Model formulation, Journal of Turbomachinery 128 (2006), 413–422
[7] Schlichting H., Gersten K.: Boundary-Layer Theory, Springer, 2003
[8] Straka P., Příhoda J.: Laminar-turbulent boundary layer transition modelling for turbomachinery flows, Czech Aerospace Proceedings 4 (2010), 10–12
[9] Walters D.K., Cokljat D.: Three-equation eddy-viscosity model for Reynolds-averaged Navier-Stokes simulations of transitional flow, Journal of Fluids Engineering 130 (2008), 121401–14
[10] Walters D.K., Leylek J.H.: A new model for boundary layer transition using a single-point RANS approach, Journal of Turbomachinery 126 (2004), 193–202

* The c_f as well as the Reynolds number Re_x was related to local velocity magnitude $U_{0.05}(x)$ at $y = 0.05\,\mathrm{m}$.

[11] Walters D.K., Leylek J.H.: Computational fluid dynamics study of wake-induced transition on a compressor-like flat plate, Journal of Turbomachinery 127 (2005), 52–63
[12] Wilcox D.C.: Turbulence Modeling for CFD, second edition ed, DCW Industries, Inc., 1998
[13] Zheng X., Liu C., Liu F., Yang C.-I.: Turbulent transition simulation using the k-ω model, Int. J. Numer. Meth. Engng. 42 (1998), 907–926

Received in editor's office: September 11, 2012
Approved for publishing: August 26, 2013